Stress response and detoxification mechanisms involved in non-target site herbicide resistance in sunflower

Tatiana Vega*[1*], Mercedes Gil*[1*], Gabriela Martin[1], Sebastián Moschen[2,3], Liliana Picardi[4], Graciela Nestares[1]

[1]Instituto de Investigaciones en Ciencias Agrarias, Facultad de Ciencias Agrarias, Universidad Nacional de Rosario-CONICET. Campo Experimental "José Villarino", S2125ZAA, Zavalla, Santa Fe, Argentina.

[2]Estación Experimental Agropecuaria Famaillá, Instituto Nacional de Tecnología Agropecuaria, Famaillá, Tucumán, Argentina.

[3]Consejo Nacional de Investigaciones Científicas y Técnicas, Ciudad Autónoma de Buenos Aires, Argentina.

[4]Consejo de Investigaciones de la Universidad Nacional de Rosario, Santa Fe, Argentina

[*]**Tatiana Vega and Mercedes Gil should be considered joint first authors**

Corresponding author: Tatiana Vega, Instituto de Investigaciones en Ciencias Agrarias (IICAR), Facultad de Ciencias Agrarias, Universidad Nacional de Rosario-CONICET. Campo Experimental "José Villarino", S2125ZAA, Zavalla, Santa Fe, Argentina.

vega@iicar-conicet.gob.ar

This article has been accepted for publication and undergone full peer review but has not been through the copyediting, typesetting, pagination and proofreading process, which may lead to differences between this version and the Version of Record. Please cite this article as doi: 10.1002/csc2.20138.

Abstract

The nature of non-target-site imidazolinone herbicide resistance (NTSR) in HA425 sunflower has not yet been fully characterized but could be related to xenobiotic metabolism. The objective of this study was to evaluate the role of cytochrome P450 monooxygenases (P450s) and other detoxification-related proteins in NTSR in sunflower. Two sunflower inbred lines were used: HA 425, which is imidazolinone (IMI)-resistant (Imisun), and HA 89, which is IMI-susceptible. The growth response to the IMI herbicide imazethapyr in combination with the P450 inhibitors 1-aminobenzotriazole (ABT) or piperonyl butoxide (PBO) was evaluated in 15-day-old sunflower plantlets. Roots were collected, and label-free quantitation (LFQ) proteomic analysis was carried out to characterize the NTSR mechanisms involved in the IMI resistance trait in sunflower. The increased phytotoxicity of imazethapyr observed in the resistant line when ABT or PBO were present agrees with the hypothesis that NTSR mechanisms may contribute to herbicide resistance in sunflower. The herbicide treatment also led to changes in the levels of biotic and abiotic stress-related proteins, glutathione S-transferases and cytochrome P450s, among others. Plant growth and root protein expression response to IMI herbicides in sunflower would be a combination of stress-related and detoxification mechanisms. Understanding the basis of NTSR becomes helpful to exploit this trait in sunflower crop and to develop xenobiotic-resistant, soil-remediating cultivars.

Keywords: plant growth response - label-free quantitative proteomics – sunflower – non-target-site herbicide resistance – imazethapyr

Abbreviations: ABC: ATP-binding cassette; ABT: 1-aminobenzotriazole; AHAS: acetohydroxyacid synthase; GSTs: glutathione S-transferases; IMI: imidazolinones; LFQ:

label-free quantitation; MS: mass spectrometry; NTSR: non-target-site resistance; P450: cytochrome P450 monooxygenases; PBO: piperonyl butoxide; ROS: reactive oxygen species; TSR: target-site resistance.

1 INTRODUCTION

Plant response to environmental stresses such as drought, cold and xenobiotics is mediated by the regulation of gene expression. A major abiotic stress encountered by cultivated sunflower (*Helianthus annuus* L.) is the application of several classes of herbicides, including imidazolinones (IMIs). In IMI-sensitive dicot plants such as sunflower, this group of herbicides inhibits acetohydroxyacid synthase (AHAS) (E.C.4.1.3.18), also called acetolactate synthase, an enzyme that catalyzes the first reaction in the biosynthetic pathway of branched-chain amino acids (Duggleby et al., 2008).

In 1998, Al-Khatib et al. obtained a wild sunflower (*Helianthus annuus* L.) population resistant to IMI (PUR *H. annuus*) (Al-Khatib et al., 1998). These researchers introgressed the herbicide resistance trait into sunflower elite inbred lines by conventional breeding methods, developing IMI-resistant cultivars known as Imisun sunflowers (Miller and Al-Khatib, 2002; Sala et al., 2012). The incorporation of the IMI resistance trait in sunflower represented a major step in weed control and productivity improvement in this crop.

In addition to target-site resistance (TSR) mechanisms, Imisun sunflowers present non-target-site resistance (NTSR) to IMI herbicides (Breccia et al., 2017; Gil et al., 2018a,b; Sala et al., 2012). Although TSR mechanisms in sunflower are well described (Breccia et al., 2013; Kolkman et al., 2004; Sala et al., 2012; Vega et al., 2009, 2012), the nature of NTSR mechanisms has not yet been fully characterized but could be related to xenobiotic metabolism (Gil and Nestares, 2019). Generally, NTSR involves polygenic control (Busi et

al., 2011; Petit et al., 2010), arises from stress response pathways already present in the plant (Délye, 2012), and includes constitutive and inducible effectors that develop resistance to herbicides with multiple modes of action. NTSR mechanisms consist of a reduction in herbicide penetration and translocation, an enhanced herbicide degradation (metabolic resistance), and/or a protection against the collateral damage of herbicide action (Délye, 2012; Duhoux et al., 2017). These metabolic resistance processes have been related with several gene families, including cytochrome P450 monooxygenases (P450s), glutathione S-transferases (GSTs), glycosyltransferases, and ATP-binding cassette (ABC) transporters (Délye, 2012; Manabe et al., 2007; Yuan et al., 2007).

In particular, P450s have been shown to be involved in the metabolism of different types of herbicides in several crops and weed species (Siminszky, 2006; Yu and Powles, 2014) by carrying out *in vivo* experiments using P450 inhibitors such as tetcyclacis, 1-aminobenzotriazole (ABT), piperonyl butoxide (PBO) and malathion (Beckie and Tardif, 2012; Letouzé and Gasquez, 2003; Yang et al., 2016). Previous studies involving plant growth response and transcriptomic analysis have described the participation of P450s and other gene families in the metabolism of herbicides in the genus *Helianthus* (Balabanova et al., 2018; Breccia et al., 2017; Didierjean et al., 2002; Gil et al., 2018a,b; Kaspar et al., 2011). The high number of P450s, GSTs, ABCs and other detoxification gene families present in plant genomes increase the complexity of their individual characterization. In this context, high-throughput techniques such as global genome, transcriptome and proteome sequencing represent a chance to decipher the complex genetic control in NTSR and to identify major genes at large scale (Gil and Nestares, 2019). Combining data provided by transcriptomic, proteomic and metabolomic experiments may allow better understanding of some important physiological and molecular mechanisms unique to sunflower (Dimitrijevic and Horn, 2018).

Proteomic approaches have been found to be very helpful to understand cell responses to external stimuli (Ahmad et al., 2016) and have become a powerful tool to visualize changes in gene expression. However, they cannot always explain the regulation in protein function or plant cell metabolic changes (Tétard-Jones et al., 2018). In this regard, mass-spectrometry (MS)-based proteomic studies constitute a promising technology not only for the identification of a large group of proteins and metabolites, but also for their comparative quantitation (Cox et al., 2014). More specifically, the emergence of the statistically robust label-free quantitative (LFQ) technique has transformed quantitative proteomics research because it has allowed the simultaneous analysis of several samples (Ghosh and Xu, 2014). In recent studies, MS-based proteomic approaches have been used to describe the effects of herbicide treatment on plants and other photosynthetic organisms (Burns et al., 2017; Nestler et al., 2012; Qian et al., 2015). The present work describes the first LFQ proteomic approach to characterize the NTSR mechanisms involved in the IMI resistance trait in sunflower.

The aims of this work were: (i) to evaluate the growth response to imazethapyr in combination with two P450s inhibitors and (ii) to analyze the root protein expression response to imazethapyr in both IMI-resistant and IMI-susceptible sunflower plants.

2 MATERIALS AND METHODS

2.1 Plant growth evaluation in response to imazethapyr alone or in combination with P450 inhibitors

Two near isogenic sunflower lines were used: HA 425, classified as IMI-resistant, and HA 89, classified as IMI-susceptible. HA 425 is a BC2F6 maintainer line resulting from the cross between HA 89*3 and PUR *H. annuus* (Miller and Al-Khatib, 2002), whereas HA 89 is a

traditional inbred line developed and released by the USDA. ABT and PBO were used as P450 inhibitors. Each P450 inhibitor was evaluated in an independent assay.

. Seed was sown into individual plastic pots (70 cm^3) filled with commercial perlite. The pots were watered by capillarity with nutritive solution consisting in 1.1 g L^{-1} Murashige and Skoog´s salts (Murashige and Skoog, 1962) and incubated at 25 ± 2 °C with a 12 h photoperiod (100 µmol m^{-2} s^{-1}). After 7 days, the plants were treated with 0, 3.3, 6.6 or 20 µM of imazethapyr alone or in combination with ABT 70 µM and PBO 50 µM added to the nutritive solution. The treatment with each P450 inhibitor began 24 h before herbicide application (Breccia et al., 2017). Plants were allowed to grow until day 15 (V2 stage) and then dissected for image scanning. Total leaf area was analyzed with the Tomato Analyzer software (Rodríguez et al., 2010), while primary root length and longest lateral root length were analyzed using the ImageJ software (Abramoff et al., 2004).

The design was a randomized complete block with three replications and each experimental unit consisted of 10 plants. The assumptions of normality and homogeneity of variance were verified using Shapiro-Wilk test and Bartlett´s test, respectively. Data were subjected to a two-way analysis of variance (ANOVA)model considering imazethapyr (I) and P450 inhibitor (PI) as fixed factors. The effect of each P450 inhibitor was assessed using orthogonal contrasts ($p < 0.05$) for each herbicide concentration. Statistical analysis was carried out using the R software (R Core Team, 2018).

When the orthogonal contrast was significant, the variable reduction percentage as a result of the inhibitor treatment was calculated, as follows: [(imazethapyr – imazethapyr + inhibitor)/imazethapyr] × 100 (Beckie et al., 2012; Breccia et al., 2017).

2.2 LFQ studies in sunflower roots

Roots of plants at the V2 stage treated with 0 (control) or 3.3 µM imazethapyr for the last 7 days were frozen in liquid nitrogen. Ten plants per treatment and three technical replicates were used in this experiment. Proteins were extracted as described in Wu et al. (2014) from 1 g root tissue per genotype/treatment combination. Total protein concentration was quantified by the method of Bradford (1976). Then, 50-µg aliquots of each sample were precipitated using trichloroacetic acid (TCA, 100 %) at a final concentration of 2 % W/V, washed in 80 % chilled acetone, and air-dried. Pellets were dissolved in 100 µL 6 M urea for protein denaturation and then reduced with 10 mM dithiothreitol at 56 ºC for 45 min. Next, the samples were treated with 20 mM iodoacetamide for 45 min in the dark to avoid the reformation of disulfide bonds and finally precipitated in 20 % TCA (100 %). Pellets were sent to the CEQUIBIEM Proteomics Facility (Universidad de Buenos Aires, Buenos Aires, Argentina) for protein digestion and MS analysis. There, each sample was resuspended in 50 mM ammonium bicarbonate pH 8, overnight digested with sequencing-grade modified trypsin (Promega) and salt-cleaned with Zip-Tip C18 (Merck Millipore). Desalted peptides were analyzed by nanoHPLC (EASY-nLC 1000, ThermoScientific, Germany) coupled to an Orbitrap technology mass spectrometer (Q-Exactive, High Collision Dissociation cell and Orbitrap analyzer, ThermoScientific, Germany). Peptide ionization was performed by electrospray (Easy Spray, Thermo Scientific) at 2.5kV. MS-data were analyzed by the Proteome Discoverer 2.1 software (ThermoScientific, Germany) using peptide peak area for identification against the sunflower genome sequencing data (Badouin et al., 2017) and a set of commonly observed contaminants. Search was performed using the following search parameters: up to two missed cleavages allowed, precursor ion mass tolerance 10 ppm, and fragmentation mass tolerance of 0.05 Da. Acetylation (N-term) and oxidation (M) were used as dynamic modifications; carbamidomethylation (C) was used as static modification with 1 % false discovery rate. The relative abundance of peptides across treatments was compared

using the Perseus Software (Tyanova et al., 2016). Functional categorization was performed using the MapMan library (Usadel et al., 2005) generated via the Mercator annotation pipeline (Lohse et al., 2014). Protein abundance was visualized using the MapMan software (version 3.6.0RC1) (Schulze and Usadel, 2010; Thimm et al., 2004). The MS proteomics data were deposited at the ProteomeXchange Consortium via the PRIDE (Perez-Riverol et al., 2019) partner repository with the dataset identifier PXD014689.

3 RESULTS

3.1 Plant growth response after treatment with imazethapyr alone or in combination with P450 inhibitors

Total leaf area, primary root length, and longest lateral root length were evaluated in both the HA 425 (resistant) and HA 89 (susceptible) sunflower lines after 7 days of treatment with 0, 3.3, 6.6 or 20 µM imazethapyr (Fig. 1) in combination with ABT or PBO.

The ANOVA showed that imazethapyr affected all the evaluated traits of both genotypes (Supplemental Tables S1-4). There was a significant ($p < 0.05$) interaction effect between imazethapyr and PBO in the longest lateral root length for HA 425 resistant line (Supplemental Table S1). In addition, ABT treatment affected the primary root length and longest lateral root length in HA 425 (Supplemental Table S3).

According to orthogonal contrast analysis, neither PBO nor ABT had effect on any variable for the HA 89 line (Table 1). This susceptible line was greatly affected by herbicide application. The orthogonal contrast analysis also showed significant reduction in the primary root length in the HA 425 resistant line after 20 µM imazethapyr + ABT treatment, with a variable reduction percentage of 13.35 % (Table 1). This line also showed a reduction of

10.61 % in the longest lateral root length after ABT treatment and a reduction of 23.14 % after 3.3 μM imazethapyr + PBO treatment (Table 1).

3.2 Optimal concentration of imazethapyr for proteomic analysis

The optimal concentration of imazethapyr was determined by analyzing foliar damage levels after herbicide treatment. At the optimal concentration, herbicide-resistant plants should exhibit 100 % survival with no visible damage after 7 days of treatment, while susceptible plants should show high damage levels. In our study, at 3.3 μM imazethapyr, the HA 425 line showed no phytotoxic symptoms, whereas the HA 89 line was highly damaged (Fig. 1). Moreover, as a result of the 3.3 μM imazethapyr + PBO treatment, the HA 425 line showed a significant reversal of the resistance level (Table 1), indicating that, at this concentration, P450s are already participating in detoxifying the herbicide. Thus, according to these results, the optimal concentration of imazethapyr for proteomic analysis was 3.3 μM.

3.3 LFQ studies in sunflower roots

Differentially expressed proteins between control and herbicide-treated roots were classified as up-regulated or down-regulated according to the average change (herbicide-treated/control ratio) value. Up-regulated proteins presented an average change > 2-fold.

A total of 2578 peptides were identified in the HA 425 line, 46 of which were up-regulated (Table 2) and 20 of which were down-regulated (Supplemental Table 5), whereas a total of 2863 peptides were identified in the HA 89 line, 88 of which were up-regulated (Table 3) and 85 of which were down-regulated (Supplemental Table 6).

In both lines, imazethapyr treatment resulted in enhanced expression of proteins involved in several metabolic pathways such as cell wall biosynthesis and modification (expansins, extensins, lignin metabolism-related and cell wall-degrading proteins), pathogen and biotic

stress (chitinases, pathogen response (PR)-proteins), abiotic stress, reactive oxygen species (ROS) production and heavy metal response. This suggests that herbicide treatment triggers stress response mechanisms. In addition, the herbicide induced primary metabolism, pentose-phosphate shunt, tricarboxylic acid cycle, and carbohydrate metabolism upregulation, all of which indicate a high energy demand under herbicide stress conditions. The increased expression levels of t-RNA-related and ribosomal polypeptides could also be related to enhanced protein synthesis, which is a general response to stress. Detoxification pathways via GSTs and glycosyltransferases were up-regulated in both genotypes, whereas P450s were up-regulated in the HA 425 line, suggesting the presence of early xenobiotic metabolism in roots.

4 DISCUSSION

IMI herbicides such as imazethapyr are generally applied by spraying at the field and a significant amount reaches the soil surface, providing a continuous supply of sub-lethal doses of the herbicide via the roots. Therefore, the active concentration of herbicide in the plant is a balance between the foliar uptake, the soil uptake and the effective number of molecules that reach the target enzyme.

Previously, NTSR mechanisms involved in imazapyr resistance have been found to be related to P450s (Breccia et al., 2017) in Imisun genotypes. In the present study, we performed whole-plant *in vivo* analyses using two different P450 inhibitors to determine the participation of these enzymes in imazethapyr resistance in Imisun sunflowers. In the HA 425 resistant line, the variable reduction percentage in the longest lateral root length as a result of PBO treatment was estimated to be 23 %. In addition, the variable reduction percentages in the longest lateral root length and primary root length after ABT treatment were 11 % and 13 %, respectively. These results suggest different P450s specificity towards the different

inhibitors in sunflower. P450s isozymes are differently expressed between tissues (Siminszky 2006). Breccia et al. (2017) observed a reduction in leaf area after imazapyr and PBO treatment in HA 425 line while both PBO and ABT caused a reduction in the lateral root growth. On the other hand, increased herbicide toxicity after P450s inhibitor malathion treatment was detected on shoot length but not on root length at seedling stage in a sunflower line (Kaspar et al. 2011). The P450s isozymes evaluated in this study were particularly active in roots. Increased herbicide phytotoxicity levels after the treatment with the P450 inhibitors were only detected in the HA 425 resistant line. These results suggest that a P450-detoxification mechanism involved in herbicide resistance could be present in Imisun sunflowers. This NTSR mechanism mediated by P450s that are particularly inhibited by ABT and PBO would enhance herbicide resistance in this species.

Recent transcriptomic characterization by cDNA-amplified fragment length polymorphism has allowed detecting sequences related to imazethapyr metabolism in sunflower leaves that corresponded to four gene families: ABC transporters, glycosyltransferases, P450s and UDP-glucuronosyl/UDP-glucosyltransferases (Gil et al., 2018b). In addition, RNA-Seq analysis has allowed identifying detoxification genes potentially related to imazethapyr resistance in sunflower: cytochrome P450 monooxygenases, ABC transporters, UDP-glucuronosyl/UDP-glucosyltransferases, glycosyltransferases and GSTs (Gil et al., 2018a). These herbicide-detoxifying genes show no differential expression between control and imazethapyr-treated leaves at RNA level, supporting the hypothesis that herbicide metabolism in Imisun sunflower is constitutive (Gil et al., 2018a). In addition, the protein profiles of IMI-resistant herbicide-treated roots showed an increased expression of xenobiotic metabolism enzymes such as UDP-glycosyltransferases, GSTs and cytochrome P450s. A similar response was observed by Qian et al. (2015) in IMI-treated *Arabidopsis thaliana* roots. Moreover, several members of the P450 protein family have been shown to be related to AHAS-inhibiting

herbicide resistance in rice (Saika et al., 2014), *Echinochloa* sp. (Iwakami et al., 2014) and *Lollium* sp.(Duhoux and Délye 2013; Duhoux et al., 2015). In the present study, P450 protein CYP71D8 was found to be up-regulated in the herbicide-treated roots of the resistant genotype, in coincidence with the results obtained by Zhao et al. (2017) in mesosulfuron-methyl resistant *Alopecurus aequalis*. Further validation studies such as in situ detection and imazethapyr-associated metabolites analysis would be appropriate to better understand the involvement of CYP71D8 in NTSR in Imisun sunflower.

Some GST genes conferring herbicide resistance have been identified in crop species such as maize (*Zea mays* L.) (Karavangeli et al., 2005), wheat (*Triticum aestivum*) (Thom et al., 2002) and soybean (*Glycine max*) (Skipsey et al., 2005). Although several GSTs have been described, only the Thau (U) and Phi (F) classes are involved in plant herbicide detoxification (Cummins et al., 2011). In our work, herbicide-resistant and herbicide-susceptible plant roots presented up-regulated expression levels of Thau-class GSTs. Thau-class GSTs are present only in vascular plants and are primarily responsible for herbicide detoxification in crops (Labrou et al., 2015). In herbicide-resistant weeds, Thau-class GSTs have been associated with NTSR to acetyl coenzyme A carboxylase and AHAS-inhibiting herbicides (Duhoux et al., 2015; Gaines et al., 2014).

Plant stress characterization by proteomic approaches allows identifying potential candidate genes to develop biotic and abiotic stress-resistant plants (Ahmad et al., 2016). In sunflower, several proteomic studies have been performed to evaluate the response to drought (Castillejo et al., 2008; Fulda et al., 2011; Ghaffari et al., 2013, 2017), cold (Balbuena et al., 2011) and metal stress (Garcia et al., 2006, 2009; Lopes Júnior et al., 2015; Printz et al., 2013). The present work describes the first proteomic approach designed for the characterization of IMI-resistance mechanisms in sunflower and contributes to a better understanding of crop response to xenobiotics.

5 CONCLUSION

The whole-plant *in vivo* analyses carried out in this study suggest that a NTSR mechanism mediated by P450 isozymes particularly inhibited by PBO and ABT contributes to imazethapyr resistance in Imisun sunflower. In addition, stress-related proteins were associated with the response to the imazethapyr in both resistant and susceptible genotypes while cytochrome P450 proteins were up-regulated only in the resistant line. These results strengthen the hypothesis that NTSR mechanisms are involved in IMI resistance in Imisun sunflower and also reveal the contribution of biotic and abiotic stress-related proteins to this trait.

6 ACKNOWLEDGMENTS

We thank Dr Jerry Miller and Dr José María Bruniard for kindly providing the seed materials. This work was supported by grants from FONCyT (PICT 2013-1010) and Consejo Nacional de Investigaciones Científicas y Técnicas (CONICET, Proyecto P-UE 22920160100043), Argentina.

7 REFERENCES

Abramoff, M.D., Magalhães, P.J., Ram, S.J. 2004. Image processing with ImageJ. Biophotonics Int. 11(7):36–42.

Ahmad, P., Latef, A.A.H.A., Rasool, S., Akram, N.A., Ashraf, M., Gucel, S. 2016. Role of proteomics in crop stress tolerance. Front. Plant Sci. 7:1336.

Al-Khatib, K., Baumgartner, J.R., Peterson, D.E., Currie, R.S. 1998. Imazethapyr resistance in common sunflower (*Helianthus annuus*). Weed Sci. 46(4):403–407.

Badouin, H., Gouzy, J., Grassa, C.J., Murat, F., Staton, S.E., et al. 2017. The sunflower genome provides insights into oil metabolism, flowering and Asterid evolution. Nature 546(7656):148–152.

Balabanova, D., Remans, T., Vassilev, A., Cuypers, A., Vangronsveld, J. 2018. Possible involvement of glutathione S-transferases in imazamox detoxification in an imidazolinone-resistant sunflower hybrid. J. Plant Physiol. 221:62–65.

Balbuena, T.S., Salas, J.J., Martínez-Force, E., Garcés, R., Thelen, J.J. 2011. Proteome analysis of cold acclimation in sunflower. J. Proteome Res. 10(5):2330–2346.

Beckie, H.J., Tardif, F.J. 2012. Herbicide cross resistance in weeds. Crop Prot. 35:15–28.

Beckie, H.J., Warwick, S.I., Sauder, C.A. 2012. Basis for herbicide resistance in canadian populations of wild oat (*Avena fatua*). Weed Sci. 60(01):10–18.

Bradford, M.M. 1976. A rapid and sensitive method for the quantitation of microgram quantities of protein utilizing the principle of protein-dye binding. Anal. Biochem. 72(1–2):248–254.

Breccia, G., Gil, M., Vega, T., Altieri, E., Bulos, M., et al. 2017. Contribution of non-target-site resistance in imidazolinone-resistant imisun sunflower. Bragantia. 76(4):536–42.

Breccia, G., Vega, T., Felitti, S.A., Picardi, L., Nestares, G. 2013. Differential expression of acetohydroxyacid synthase genes in sunflower plantlets and its response to imazapyr herbicide. Plant Sci. 208:28-33.

Burns, E.E., Keith, B.K., Refai, M.Y., Bothner, B., Dyer, W.E. 2017. Proteomic and biochemical assays of glutathione-related proteins in susceptible and multiple herbicide resistant *Avena fatua* L . Pestic. Biochem. Physiol. 140:69–78.

Busi, R., Vila-Aiub, M.M., Powles, S.B. 2011. Genetic control of a cytochrome P450 metabolism-based herbicide resistance mechanism in *Lolium rigidum*. Heredity. 106(5):817–824.

Castillejo, M.A., Maldonado, A.M., Ogueta, S., Jorrin, J. V. 2008. Proteomic analysis of responses to drought stress in sunflower (*Helianthus annuus*) leaves by 2DE gel electrophoresis and mass spectrometry. Open Proteomics J. 1(1):59–71.

Cox, J., Hein, M.Y., Luber, C.A., Paron, I., Nagaraj, N., Mann, M. 2014. Accurate proteome-wide label-free quantification by delayed normalization and maximal peptide ratio extraction, termed MaxLFQ. Mol. Cell. Proteomics. 13(9):2513–2526.

Cummins, I., Dixon, D.P., Freitag-Pohl, S., Skipsey, M., Edwards, R. 2011. Multiple roles for plant glutathione transferases in xenobiotic detoxification. Drug Metab. Rev. 43(2):266–280.

Délye, C. 2012. Unravelling the genetic bases of non-target-site-based resistance (NTSR) to herbicides: A major challenge for weed science in the forthcoming decade. Pest Manag. Sci. 69(2):176–187.

Didierjean, L., Gondet, L., Perkins, R., Lau, S.C., et al. 2002. Engineering herbicide metabolism in tobacco and Arabidopsis with CYP76B1, a cytochrome P450 enzyme from Jerusalem artichoke. Plant Physiol. 130(1):179–189.

Dimitrijevic, A., Horn, R. 2018. Sunflower hybrid breeding: from markers to genomic

selection. Front. Plant Sci. 8:2238.

Duggleby, R.G., McCourt, J.A., Guddat, L.W. 2008. Structure and mechanism of inhibition of plant acetohydroxyacid synthase. Plant Physiol. Biochem. 46(3):309–324.

Duhoux, A., Carrère, S., Duhoux, A., Délye, C. 2017. Transcriptional markers enable identification of rye-grass (*Lolium* sp.) plants with non-target-site-based resistance to herbicides inhibiting acetolactate-synthase. Plant Sci. 257:22–36.

Duhoux, A., Carrère, S., Gouzy, J., Bonin, L., Délye, C. 2015. RNA-Seq analysis of rye-grass transcriptomic response to an herbicide inhibiting acetolactate-synthase identifies transcripts linked to non-target-site-based resistance. Plant Mol. Biol. 87(4–5):473–487.

Duhoux, A., Délye, C. 2013. Reference genes to study herbicide stress response in *Lolium* sp.: Up-regulation of P450 genes in plants resistant to acetolactate-synthase inhibitors. *PLoS One*. 8(5): e63576.

Fulda, S., Mikkat, S., Stegmann, H., Horn, R. 2011. Physiology and proteomics of drought stress acclimation in sunflower (*Helianthus annuus* L.). Plant Biol. 13(4):632–642.

Gaines, T.A., Lorentz, L., Figge, A., Herrmann, J., Maiwald, F., et al. 2014. RNA-Seq transcriptome analysis to identify genes involved in metabolism-based diclofop resistance in *Lolium rigidum*. Plant J. 78(5):865–876.

Garcia, J.S., Gratão, P.L., Azevedo, R.A., Arruda, M.A.Z. 2006. Metal contamination effects on sunflower (*Helianthus annuus* L.) growth and protein expression in leaves during development. J. Agric. Food Chem. 54(22):8623–8630.

Garcia, J.S., Souza, G.H.M.F., Eberlin, M.N., Arruda, M.A.Z. 2009. Evaluation of metal-ion

stress in sunflower (*Helianthus annuus* L.) leaves through proteomic changes. Metallomics. 1(1):107–113.

Ghaffari, M., Toorchi, M., Valizadeh, M., Komatsu, S. 2013. Differential response of root proteome to drought stress in drought sensitive and tolerant sunflower inbred lines. Funct. Plant Biol. 40(6):609.

Ghaffari, M., Toorchi, M., Valizadeh, M., Shakiba, M.. 2017. Proteomic prospects for tolerance of sunflower (*Helianthus annuus*) to drought stress during the flowering stage. Crop Pasture Sci. 68(5):457–465.

Ghosh, D., Xu, J. 2014. Abiotic stress responses in plant roots: a proteomics perspective. Front. Plant Sci. 5:1–13.

Gil, M., Nestares, G. 2019. Decoding non-target-site herbicide resistance in sunflower: The beginning of the story. Helia. 42(70):1–16.

Gil, M., Nestares, G., Balzergue, S., Vega, T., Felitti, S., Picardi, L. 2018a. Characterization of non-target-site mechanisms in imidazolinone-resistant sunflower by RNA-seq. Helia. 41(69):267–278.

Gil, M., Ochogavía, A.C., Vega, T., Felitti, S.A., Nestares, G. 2018b. Transcript profiling of non-target-site imidazolinone resistance in imisun sunflower. Crop Sci. 58(5):1991–2001.

Iwakami, S., Uchino, A., Kataoka, Y., Shibaike, H., Watanabe, H., Inamura, T. 2014. Cytochrome P450 genes induced by bispyribac-sodium treatment in a multiple-herbicide-resistant biotype of *Echinochloa phyllopogon.* Pest Manag. Sci. 70(4):549–558.

Karavangeli, M., Labrou, N.E., Clonis, Y.D., Tsaftaris, A. 2005. Development of transgenic tobacco plants overexpressing maize glutathione S-transferase I for chloroacetanilide herbicides phytoremediation. Biomol. Eng. 22(4):121–128.

Kaspar, M., Grondona, M., Leon, A., Zambelli, A. 2011. Selection of a sunflower line with multiple herbicide tolerance that is reversed by the P450 inhibitor malathion. Weed Sci. 59(2):232–237.

Kolkman, J.M., Slabaugh, M.B., Bruniard, J.M., Berry, S., Bushman, B.S., et al. 2004. Acetohydroxyacid synthase mutations conferring resistance to imidazolinone or sulfonylurea herbicides in sunflower. Theor. Appl. Genet. 109(6):1147–1159.

Labrou, N.E., Papageorgiou, A.C., Pavli, O., Flemetakis, E. 2015. Plant GSTome: Structure and functional role in xenome network and plant stress response. Curr. Opin. Biotechnol. 32:186–194.

Letouzé, A., Gasquez, J. 2003. Enhanced activity of several herbicide-degrading enzymes: a suggested mechanism responsible for multiple resistance in blackgrass (*Alopecurus myosuroides* Huds.). Agronomie. 23:601–608.

Lohse, M., Nagel, A., Herter, T., May, P., Schroda, M., et al. 2014. Mercator : a fast and simple web server for genome scale functional annotation of plant sequence data. Plant, Cell Environ. 37:1250–1258.

Lopes Júnior, C.A., Barbosa, H. de S., Moretto Galazzi, R., Ferreira Koolen, H.H., Gozzo, F.C., Arruda, M.A.Z. 2015. Evaluation of proteome alterations induced by cadmium stress in sunflower (*Helianthus annuus* L.) cultures. Ecotoxicol. Environ. Saf. 119:170–177.

Manabe, Y., Tinker, N., Colville, A., Miki, B. 2007. CSR1, the sole target of imidazolinone herbicide in *Arabidopsis thaliana.* Plant Cell Physiol. 48(9):1340–1358.

Miller, J.F., Al-Khatib, K. 2002. Registration of imidazolinone herbicide-resistant sunflower maintainer (HA 425) and fertility restorer (RHA 426 and RHA 427) germplasms. Crop Sci. 42:988–989.

Murashige, T., Skoog, F. 1962. A revised medium for rapid growth and bio assays with tobacco tissue cultures. Physiol. Plant. 15(3):473–497.

Nestler, H., Groh, K.J., Schönenberger, R., Eggen, R.I.L., Suter, M.J. 2012. Linking proteome responses with physiological and biochemical effects in herbicide-exposed *Chlamydomonas reinhardtii.* J. Proteomics. 75(17):5370–5385.

Perez-Riverol, Y., Csordas, A., Bai, J., Bernal-Llinares, M., Hewapathirana, S., et al. 2019. The PRIDE database and related tools and resources in 2019: Improving support for quantification data. Nucleic Acids Res. 47:D442–450.

Petit, C., Duhieu, B., Boucansaud, K., Délye, C. 2010. Complex genetic control of non-target-site-based resistance to herbicides inhibiting acetyl-coenzyme A carboxylase and acetolactate-synthase in *Alopecurus myosuroides* Huds. Plant Sci. 178(6):501–509.

Printz, B., Sergeant, K., Guignard, C., Renaut, J., Hausman, J.F. 2013. Physiological and proteome study of sunflowers exposed to a polymetallic constraint. Proteomics. 13:1993–2015.

Qian, H., Lu, H., Ding, H., Lavoie, M., Li, Y., et al. 2015. Analyzing *Arabidopsis thaliana* root proteome provides insights into the molecular bases of enantioselective imazethapyr toxicity. *Sci. Rep.* 5:1–13.

R Core Team. 2018. R: A language and environment for statistical computing. R Found. Stat. Comput., Vienna.

Rodríguez, G.R., Moyseenko, J.B., Robbins, M.D., Huarachi Morejón, N., Francis, D.M., van der Knaap, E. 2010. Tomato Analyzer: a useful software application to collect accurate and detailed morphological and colorimetric data from two-dimensional objects. J. Vis. Exp. (37):1–11.

Saika, H., Horita, J., Taguchi-Shiobara, F., Nonaka, S., Nishizawa-Yokoi, A., et al. 2014. A novel rice cytochrome P450 gene, CYP72A31, confers tolerance to acetolactate synthase-inhibiting herbicides in rice and Arabidopsis. Plant Physiol. 166(3):1232–1240.

Sala, C.A., Bulos, M., Altieri, E., Ramos, M.L. 2012. Sunflower: improving crop productivity and abiotic stress tolerance. In: Tuteja, N., Singh Gill, S., Tiburcio, A.F., Tuteja, R., editors, Improving Crop Resistance to Abiotic Stress. John Wiley & Sons, USA, pp. 1203–1249.

Schulze, W.X., Usadel, B. 2010. Quantitation in mass-spectrometry-based proteomics. Annu. Rev. Plant Biol. 61(1):491–516.

Siminszky, B. 2006. Plant cytochrome P450-mediated herbicide metabolism. Phytochem. Rev. 5(2–3):445–458.

Skipsey, M., Cummins, I., Andrews, C.J., Jepson, I., Edwards, R. 2005. Manipulation of plant tolerance to herbicides through co-ordinated metabolic engineering of a detoxifying glutathione transferase and thiol cosubstrate. Plant Biotechnol. J. 3(4):409–420.

Tétard-Jones, C., Sabbadin, F., Moss, S., Hull, R., Neve, P., Edwards, R. 2018. Changes in

the proteome of the problem weed blackgrass correlating with multiple-herbicide resistance. Plant J. 94(4):709–720.

Thimm, O., Bläsing, O., Gibon, Y., Nagel, A., Meyer, S., et al. 2004. MAPMAN: A user-driven tool to display genomics data sets onto diagrams of metabolic pathways and other biological processes. Plant J. 37(6):914–939.

Thom, R., Cummins, I., Dixon, D.P., Edwards, R., Cole, D.J., Lapthorn, A.J. 2002. Structure of a tau class glutathione S-transferase from wheat active in herbicide detoxification. Biochemistry. 41(22):7008–7020.

Tyanova, S., Temu, T., Sinitcyn, P., Carlson, A., Hein, M.Y., et al. 2016. The Perseus computational platform for comprehensive analysis of (prote)omics data. Nat. Methods. 13(9):731–740.

Usadel, B., Nagel, A., Thimm, O., Redestig, H., Blaesing, O.E., et al. 2005. Extension of the visualization tool mapman to allow statistical analysis of arrays, display of coresponding genes, and comparison with known responses. Plant Physiol. 138(3):1195–1204.

Vega, T., Breccia, G., Gil, M., Zorzoli, R., Picardi, L., Nestares, G. 2012. Acetohydroxyacid synthase (AHAS) in vivo assay for screening imidazolinone-resistance in sunflower (*Helianthus annuus* L.). Plant Physiol. Biochem. 61:103-107.

Vega, T., Breccia, G., Nestares, G., Mayor, M.L., Zorzoli, R., Picardi, L. 2009. Soil-less bioassays for early screening for resistance to imazapyr in sunflower (*Helianthus annuus* L.). Pest Manag. Sci. 65(9):991–995.

Wu, X., Xiong, E., Wang, W., Scali, M., Cresti, M.. 2014. Universal sample preparation method integrating trichloroacetic acid/acetone precipitation with phenol extraction for

crop proteomic analysis. Nat. Protoc. 9(2):362–374.

Yang, Q., Deng, W., Li, X., Yu, Q., Bai, L., Zheng, M. 2016. Target-site and non-target-site based resistance to the herbicide tribenuron-methyl in flixweed (*Descurainia sophia* L.). BMC Genomics. 17:551–563.

Yu, Q., Powles, S. 2014. Metabolism-based herbicide resistance and cross-resistance in crop weeds: a threat to herbicide sustainability and global crop production. Plant Physiol. 166(3):1106–1118.

Yuan, J.S., Tranel, P.J., Stewart, C.N. 2007. Non-target-site herbicide resistance: a family business. Trends Plant Sci. 12(1):6–13.

Zhao, N., Li, W., Bai, S., Guo, W., Yuan, G., et al. 2017. Transcriptome profiling to identify genes involved in mesosulfuron-methyl resistance in *Alopecurus aequalis.* Front. Plant Sci. 8:1–16.

Fig. 1 Foliar phytotoxic symptoms in sunflower plants at the V2 stage treated with imazethapyr for 7 days. HA 425 (IMI-resistant line) after (a) control (0 µM) and (b) 3.3 µM imazethapyr; HA 89 (IMI-susceptible line) after (c) control (0 µM) and (d) 3.3 µM imazethapyr.

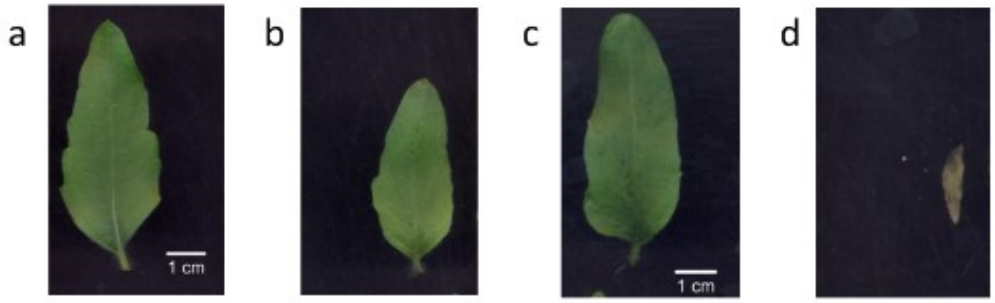

TABLE 1 Mean values of evaluated trait for each treatment combination in HA 89 susceptible and HA 425 resistant lines

Genotype	**Imazethapyrrate** (μM)	**P450 inhibitor**	**Total leaf area** (cm^2)	**Primary root length** (cm)	**Longest lateral root length** (cm)
HA 89	0	ABT 0 μM	20.19	7.85	5.09
		ABT 70 μM	18.65	7.59	4.94
	3.3	ABT 0 μM	1.20	7.74	4.24
		ABT 70 μM	1.13	7.08	4.35
	6.6	ABT 0 μM	1.02	7.36	4.50
		ABT 70 μM	0.91	7.50	4.06
	20	ABT 0 μM	0.78	6.40	3.88
		ABT 70 μM	0.86	6.19	4.09
	0	PBO 0 μM	20.53	6.73	5.19
		PBO 50 μM	21.28	7.07	5.11
	3.3	PBO 0 μM	0.90	6.24	4.43
		PBO 50 μM	1.10	7.09	4.07
	6.6	PBO 0 μM	1.28	6.83	3.74

		PBO 50 µM	1.10	5.65	3.70
	20	PBO 0 µM	1.07	6.06	2.74
		PBO 50 µM	1.21	4.70	1.97
HA 425	0	ABT 0 µM	12.92	8.69	5.38
		ABT 70 µM	12.03	8.51	5.20
	3.3	ABT 0 µM	7.52	8.58	4.75
		ABT 70 µM	6.78	7.47	4.67
	6.6	ABT 0 µM	5.02	7.82	**4.55 a**†
		ABT 70 µM	4.42	7.25	**4.06 b** (10.61)
	20	ABT 0 µM	4.04	**7.84 a**	4.58
		ABT 70 µM	3.03	**6.79 b** (13.35)	4.30
	0	PBO 0 µM	20.84	9.57	5.19
		PBO 50 µM	20.18	10.13	5.77
	3.3	PBO 0 µM	13.74	7.80	**5.60 a**
		PBO 50 µM	12.37	7.42	**4.30 b** (23.14)
	6.6	PBO 0 µM	7.70	6.84	4.36
		PBO 50 µM	7.02	5.96	4.02
	20	PBO 0 µM	4.80	7.16	4.33
		PBO 50 µM	4.54	5.38	3.95

†Bolded data followed by a different letter within a column and trait indicate significant differences ($p < 0.05$) between untreated plants and those treated with one of the P450 inhibitors. Data in parenthesis indicate the % reduction registered in treated plants.

TABLE 2 Differentially expressed proteins between imazethapyr-treated (I) and control (C) roots in the HA 425 line after 7 days of treatment. Only up-regulated proteins (I/C ratio > 2) are shown.

Sunflower ID	Arabidopsis ID	I/C Ratio	Protein Description
Pentose shunt			
hanxrqchr16g0529531	at2g01140	11.819	Fructose-bisphosphate aldolase activity
Fermentation			
hanxrqchr14g0432021	at1g22430	2.176	GroES-like zinc-binding dehydrogenase family protein
Tricarboxylic acid cycle			
hanxrqchr01g0018081	at3g60100	2.320	Citrate synthase 5
Mitochondrial electron transport			
hanxrqmtg0579581	atmg00510	2.512	NADH dehydrogenase subunit 7
Cell wall precursor synthesis and modification			
hanxrqchr12g0375821	at3g02570	2.108	Mannose-6-phosphate isomerase
hanxrqchr16g0500671	at2g28950	3.499	Expansin
Lipid /glycerol metabolism			
hanxrqchr08g0218541	at3g10370	2.518	Mitochondrial FAD-dependent glycerol-3-phosphate dehydrogenase
Amino acid synthesis			
hanxrqchr01g0027801	at2g36880	5.743778	S-adenosylmethionine synthase 3
Amino acid degradation			
hanxrqchr11g0331361	at4g34030	2.073	MCC-B
Secondary metabolism: phenylpropanoids			
hanxrqchr02g0034701	at3g26040	2.001	HXXXD-type acyl-transferase

Sunflower ID	Arabidopsis ID	I/C Ratio	Protein Description
hanxrqchr08g0216151	at2g33590	5.684	cinnamoyl-CoA reductase
hanxrqchr14g0444411	at4g37990	2.639	Mannitol dehydrogenase
Hormone metabolism: auxin responsive			
hanxrqchr11g0341451	at1g60710	5.692	NADP-dependent oxidoreductase
hanxrqchr14g0437351	at1g60710	2.397	Auxin-induced NADP-dependent oxidoreductase
Co-factor and vitamin metabolism			
hanxrqchr01g0007121	at5g01410	1.993	Probable pyridoxin biosynthesis protein ER1
hanxrqchr05g0159781	at5g55130	18.675	adenylyltransferase and sulfurtransferase MOCS3
Biotic stress			
hanxrqchr01g0014521	at2g38870	2.693	Putative proteinase inhibitor I13, potato inhibitor I
Abiotic stress (cold)			
hanxrqchr10g0291901	at3g53990	2.569	Adenine nucleotide alpha hydrolases-like superfamily protein
Redox: catalases			
hanxrqchr08g0216431	at4g35090	2.331	Putative catalase haem-binding site;
Xenobiotic metabolism			
hanxrqchr11g0339191	at3g46690	3.972	UDP-Glycosyltransferase superfamily protein
hanxrqchr06g0177581	at2g29420	4.205	Probable glutathione S-transferase, thau family
hanxrqchr13g0398621	at3g26300	5.724	Cytochrome P450 71D8
hanxrqchr15g0483161	at3g26300	3.171	Cytochrome P450 71D8

Sunflower ID	Arabidopsis ID	I/C Ratio	Protein Description
hanxrqchr01g0002291	at4g02860	2.021	Probable phenazine biosynthesis PhzC/PhzF protein
Misc.: Peroxidases			
hanxrqchr05g0162331	at1g71695	22.146	ATP synthase delta chain, chloroplast precursor
Misc.: dynamin			
hanxrqchr06g0168231	at3g60190	2.164	Probable DYNAMIN-like 1E
Misc.: short chain dehydrogenase/reductase (SDR)			
hanxrqchr03g0069571	at1g52340	2.696	Putative glucose/ribitol dehydrogenase
DNA: chromatin structure			
hanxrqchr05g0153181	at1g06760	5.606	Putative histone H5
DNA: unspecified			
hanxrqchr05g0158441	at5g63190	2.097	Probable MA3 domain-containing protein
Protein synthesis			
hanxrqchr15g0488241	at4g13780	2.031	Probable methionine-tRNA ligase
hanxrqchr03g0078721	at1g72550	2.205	Probable phenylalanine-tRNA ligase
hanxrqchr01g0030651	at4g10450	7.770	Probable ribosomal protein L6 family
hanxrqchr17g0564331	at3g14600	1.992	Putative 60S ribosomal protein L18a
hanxrqchr05g0142871	at1g70600	2.437	Putative ribosomal protein L18e/L15P
hanxrqchr10g0296191	at1g70600	7.480	Putative ribosomal protein L18e/L15P
Protein degradation			
hanxrqchr10g0297661	at2g14260	2.157	Probable proline iminopeptidase
hanxrqchr10g0282821	at1g03220	2.450	Probable Eukaryotic aspartyl protease
Signaling			
hanxrqchr08g0223971	at4g23160	2.148	Probable annexin A13

Sunflower ID	Arabidopsis ID	I/C Ratio	Protein Description
Cell organization			
hanxrqchr13g0405381	at1g68090	3.050	Putative annexin
hanxrqchr09g0237941	at5g20490	2.027	Probable myosin-17
hanxrqchr02g0053281	at3g11820	2.123	Probable syntaxin of plants 121
Transport proteins			
hanxrqchr13g0421951	at1g68570	2.811	Malate dehydrogenase, cytoplasmic
hanxrqchr17g0533621	at1g01620	3.430	Plasma membrane intrinsic protein 1;4
Not assigned			
hanxrqchr09g0273771	at5g61820	2.755	Putative stress up-regulated Nod 19
hanxrqchr17g0539351	at4g32930	4.675	Probable Peptidyl-tRNA hydrolase, PTH2
hanxrqchr15g0472171	at3g19990	2.770	Uncharacterized conserved protein

TABLE 3 Differentially expressed proteins between imazethapyr-treated (I) and control (C) roots in the HA 89 line after 7 days of treatment. Only up-regulated proteins (I/C ratio > 2) are shown.

Sunflower ID	Arabidopsis ID	I/C Ratio	Protein Description
Calvin cycle			
hanxrqchr16g0531101	at2g21330	2.427	Fructose-bisphosphate aldolase, chloroplast precursor
Major CHO metabolism			
hanxrqchr10g0279051	at1g43670	2.293	Inositol monophosphatase family protein
Minor CHO metabolism			
hanxrqchr09g0265471	at5g15140	3.108	Galactose mutarotase-like superfamily protein
hanxrqchr05g0136751	at5g57655	1.996	xylose isomerase family protein
hanxrqchr11g0322851	at5g08370	2.507	Alpha-galactosidase precursor
Fermentation			
hanxrqchr10g0312481	at1g54100	4.362	Aldehyde dehydrogenase family 7 member A1
Gluconeogenesis / glyoxylate cycle			
hanxrqchr03g0080571	at4g15530	10.432	Pyruvate phosphate dikinase, chloroplast precursor
OPP oxidative			
hanxrqchr03g0062861	at5g24400	3.048	Putative glucosamine/galactosamine-6-phosphate isomerase
Cell wall proteins. LRR			

Sunflower ID	Arabidopsis ID	I/C Ratio	Protein Description
hanxrqchr03g0068311	at1g62440	3.254	Putative leucine-rich repeat domain, extensin2
Cell wall degradation			
hanxrqchr10g0293191	at5g64570	2.696	Probable beta-xylosidase/alpha-L-arabinofuranosidase 2
hanxrqchr10g0319301	at3g52840	32.854	Probable beta-galactosidase
hanxrqchr13g0391131	at5g49360	18.481	Probable beta-xylosidase 1
hanxrqchr06g0170281	at3g61490	3.735	Probable polygalacturonase
Cell wall modification			
hanxrqchr03g0074761	at4g17030	2.398	Probable expansin-like B1
hanxrqchr11g0333141	at4g14130	11.480	Xyloglucan endotransglucosylase/hydrolase
hanxrqchr14g0436081	at4g14130	10.593	Probable xyloglucan endotransglucosylase/hydrolase 2
Cell wall: pectin esterases			
hanxrqchr04g0127131	at1g76160	2.579	Putative cupredoxin SKU5 similar 5 (sks5)
hanxrqchr06g0169441	at2g45220	2.509	Probable pectinesterase 2
hanxrqchr08g0212361	at1g23200	5.046	Probable plant invertase/pectin methylesterase inhibitor
hanxrqchr13g0412571	at4g19420	3.392	Probable pectinacetylesterase family protein
hanxrqchr17g0537181	at5g45280	5.035	Putative pectinacetylesterase/NOTUM
Lipid metabolism: FA synthesis and FA elongation			

Sunflower ID	Arabidopsis ID	I/C Ratio	Protein Description
hanxrqchr03g0071661	at3g05970	2.526	Probable long-chain acyl-CoA synthetase 7
Amino acid synthesis			
hanxrqchr08g0214751	at3g22200	2.528	Probable gamma aminobutyrate transaminase 3, chloroplastic
hanxrqchr14g0446441	at3g22200	2.462	Probable pyridoxal phosphate (PLP)-dependent transferase
hanxrqchr06g0170191	at3g61440	2.133	Probable L-3-cyanoalanine synthase 1, mitochondrial
Amino acid degradation			
hanxrqchr07g0197391	at3g45300	2.088	Probable isovaleryl-CoA dehydrogenase, mitochondrial
Metal handling			
hanxrqchr16g0509611	at2g40300	2.415	Ferritin-1, chloroplast precursor; Putative ferritin
Secondary metabolism			
hanxrqchr14g0434761	at4g13430	2.133	Isopropyl malate isomerase large subunit 1 (IIL1)
Hormone metabolism: ABA responsive			
hanxrqchr17g0540481	at5g13200	2.439	Probable GRAM domain family protein
hanxrqchr08g0234341	at4g27450	2.204	Probable aluminum-induced protein with YGL and LRDR motifs
hanxrqchr14g0436991	at1g60730	4.649	Putative aldo/keto reductase/potassium channel subunit beta
Hormone metabolism: Ethylene synthesis			

Sunflower ID	Arabidopsis ID	I/C Ratio	Protein Description
hanxrqchr03g0060761	at2g19590	8.242	Probable acetyl coenzyme A carboxylase oxidase 1
Hormone metabolism: Jasmonate			
hanxrqchr10g0307551	at5g42650	2.133	Probable 9-divinyl ether synthase
Biotic stress			
hanxrqchr01g0014521	at2g38870	4.665	Putative proteinase inhibitor I13, potato inhibitor I
hanxrqchr03g0092881	at3g54420	3.920	EP3 chitinase. Putative glycoside hydrolase, family 19
hanxrqchr05g0141461	at4g19810	2.817	Putative glycoside hydrolase family; Chitinase insertion domain
hanxrqchr09g0276691	at3g12500	2.467	Probable endochitinase 1
hanxrqchr15g0476701	at1g58170	2.691	Probable disease resistance-responsive (dirigent-like protein) family
hanxrqchr16g0505511	at1g19610	4.263	Predicted PR (pathogenesis-related) protein - defensin (PDF) family
Biotic stress: PR-proteins			
hanxrqchr09g0253131	at5g24090	3.195	Probable acidic endochitinase
hanxrqchr05g0161361	at1g17860	3.834	Probable kunitz family trypsin and protease inhibitor protein
hanxrqchr06g0164761	at1g17860	2.916	Putative proteinase inhibitor I3, Kunitz legume
hanxrqchr16g0506311	at1g17860	4.101	Putative proteinase inhibitor I3, Kunitz legume
Abiotic stress			

Sunflower ID	Arabidopsis ID	I/C Ratio	Protein Description
hanxrqchr03g0084471	at4g11650	2.610	Probable thaumatin-like protein
hanxrqchr09g0248171	at2g21620	3.247	RD2 - Probable adenine nucleotide alpha hydrolases-like superfamily protein
Redox: Peroxiredoxin			
hanxrqchr07g0194341	at1g48130	2.018	(glutathione peroxidase) Probable 1-Cys peroxiredoxin PER1
Misc. gluco-, galacto- and mannosidases			
hanxrqchr02g0055691	at2g28470	2.307	Probable beta-galactosidase 8
hanxrqchr15g0483951	at5g66150	2.402	Probable alpha-mannosidase, Glycosyl hydrolase family 38 protein
hanxrqchr16g0531341	at4g23160	5.326	Putative glycoside hydrolase family 38
Misc. beta 1,3 glucan hydrolases			
hanxrqchr06g0165511	at4g16260	2.832	Probable glucan endo-1,3-beta-glucosidase, vacuolar
hanxrqchr11g0351571	at4g16260	2.360	Putative glycoside hydrolase family 17
Misc. Oxidases			
hanxrqchr09g0270021	at5g56490	7.362	Putative L-gulonolactone oxidase; FAD-binding, type 2
hanxrqchr17g0552421	at5g07475	4.184	Putative cupredoxin, plastocyanin-like
Misc. nitrilases			
hanxrqchr13g0418811	at1g12570	4.347	Putative glucose-methanol-choline oxidoreductase

Sunflower ID	Arabidopsis ID	I/C Ratio	Protein Description
Misc. glutathione S transferases			
hanxrqchr06g0177581	at2g29420	2.205	Probable glutathione S-transferase, thau family
hanxrqchr16g0526541	at1g14540	4.740	Lignin-forming anionic peroxidase
Misc. peroxidases			
hanxrqchr01g0003401	at3g01190	3.516	Putative haem peroxidase, peroxidase 27-like
hanxrqchr02g0052011	at2g37130	8.185	Putative haem peroxidase, peroxidase 21, protamine P1 family
hanxrqchr03g0068911	at3g01190	2.511	Putative haem peroxidase, peroxidase 27-like
hanxrqchr10g0295991	at5g64120	19.849	Putative haem peroxidase, N-1 like
hanxrqchr10g0296231	at5g64120	4.067	Putative haem peroxidase, N-1 like
hanxrqchr12g0358371	at2g18980	2.172	Probable peroxidase superfamily protein, peroxidase 16-like
hanxrqchr14g0441921	at4g37530	3.198	Putative haem peroxidase, peroxidase 51-like
hanxrqchr17g0550071	at4g37530	2.244	Probable peroxidase superfamily protein, peroxidase 55-like
Misc. myrosinases-lectin-jacalin			
hanxrqchr02g0047121	at1g19715	4.266	Probable horcolin, mannose glucose-specific lectin-like
Misc. GDSL-motif lipase			
hanxrqchr06g0168051	at3g62280	4.036	Putative SGNH hydrolase-type esterase domain
Protein targeting. Mitochondria			

Sunflower ID	Arabidopsis ID	I/C Ratio	Protein Description
hanxrqchr10g0295691	at2g42210	15.137	Putative mitochondrial inner membrane translocase subunit
Signaling. Receptor kinases			
hanxrqchr12g0355821	at1g48480	4.211	Probable leucine-rich repeat protein kinase
hanxrqchr02g0052741	at5g49760	2.061	Probable leucine-rich repeat protein kinase family protein
hanxrqchr02g0037501	at1g56145	2.696	Probable leucine-rich repeat transmembrane protein kinase
hanxrqchr11g0331141	at1g53420	3.470	Putative serine/threonine/dual specificity protein kinase
Signaling. Calcium			
hanxrqchr02g0052431	at1g53210	2.024	Sodium calcium exchanger family calcium-binding EF hand family
Development			
hanxrqchr09g0263511	at4g37070	2.043	Probable PATATIN-like protein 5
hanxrqchr03g0087881	at4g12420	2.526	Putative cupredoxin
hanxrqchr10g0297861	at4g24220	2.738	Probable 3-oxo-Delta(4,5)-steroid 5-beta-reductase
Not assigned			
hanxrqchr01g0002291	at4g02860	2.011	Probable phenazine biosynthesis PhzC/PhzF protein
hanxrqchr03g0064561	at5g01580	2.450	Putative gamma interferon inducible lysosomal thiol reductase
hanxrqchr06g0166861	at4g10750	2.092	Probable phosphoenolpyruvate carboxylase family protein

Sunflower ID	Arabidopsis ID	I/C Ratio	Protein Description
hanxrqchr13g0407051	at3g20820	2.476	Probable leucine-rich repeat (LRR) family protein
hanxrqchr02g0033061	NR	4.377	Uncharacterized protein, supported by expression data
hanxrqchr03g0060851	NR	12.244	Putative cytolysin/lectin
hanxrqchr08g0209171	at1g07040	2.221	Uncharacterized conserved protein
hanxrqchr08g0227201	at3g21360	2.615	2-oxoglutarate (2OG) and Fe(II)-dependent oxygenase superfamily
hanxrqchr09g0273771	at5g61820	2.898	Putative stress up-regulated Nod 19
hanxrqchr11g0320871	NR	7.235	Putative actin cross-linking; Fascin; Glycoside hydrolase superfamily
hanxrqchr14g0428101	at1g31885	2.202	Uncharacterized protein, conserved in plant genome(s)
hanxrqchr14g0441831	NR	2.022	Putative rhodanese-like domain
hanxrqchr15g0492231	NR	2.305	Polyphenol oxidase precursor (chloroplast), di-copper center